



HAL
open science

Experimental analysis of hydrofoil hydroelastic trailing edge vibrations

Paul Francois, Jacques-André Astolfi, Xavier Amandolese

► **To cite this version:**

Paul Francois, Jacques-André Astolfi, Xavier Amandolese. Experimental analysis of hydrofoil hydroelastic trailing edge vibrations. 25ème Congrès Français de Mécanique, Aug 2022, Nantes, France. pp.28-35. hal-04059813

HAL Id: hal-04059813

<https://hal.science/hal-04059813>

Submitted on 5 Apr 2023

HAL is a multi-disciplinary open access archive for the deposit and dissemination of scientific research documents, whether they are published or not. The documents may come from teaching and research institutions in France or abroad, or from public or private research centers.

L'archive ouverte pluridisciplinaire **HAL**, est destinée au dépôt et à la diffusion de documents scientifiques de niveau recherche, publiés ou non, émanant des établissements d'enseignement et de recherche français ou étrangers, des laboratoires publics ou privés.

Experimental analysis of hydrofoil hydroelastic trailing edge vibrations

P. FRANCOIS^a, J-A. ASTOLFI^b, X. AMANDOLESE^c

a. IRENav, paul.francois@ecole-navale.fr

b. IRENav, jacques-andre.astolfi@ecole-navale.fr

c. LMSSC-Cnam, xavier.amandolese@lecnam.net

Résumé :

Les conditions conduisant aux vibrations hydroélastiques de bord de fuite sont étudiées sur un hydrofoil NACA0015 en Aluminium monté en configuration encastrée-libre dans un tunnel hydrodynamique. Les essais ont été menés pour des nombres de Reynolds compris entre 2×10^5 et 9×10^5 et différents angles d'incidence de 0 à 10° . De la vibrométrie laser a été utilisée pour identifier la réponse vibratoire de l'hydrofoil. De la vélocimétrie par image de particules résolue en temps (TR-PIV) a aussi été utilisée pour caractériser l'écoulement et discuter de l'origine hydrodynamique du phénomène. Ce travail a pour objectif de décrire les différentes configurations conduisant à un couplage fort entre l'écoulement et un mode d'hydrofoil caractérisé par un ventre de vibration au bord de fuite. Des amplitudes de vibration significatives ont ainsi été observées pour des angles d'incidence compris entre 3.5° et 8.5° . L'analyse de l'écoulement de bord de fuite a également révélé que le comportement de la couche limite intrados au niveau du décollement de bord de fuite joue un rôle essentiel dans le mécanisme d'excitation.

Abstract :

This paper explores the conditions for hydro-elastic trailing edge vibrations on a NACA0015 aluminium hydrofoil clamped in a hydrodynamic tunnel. Test were performed for Reynolds numbers ranging from 2×10^5 up to 9×10^5 and various angle of attack, from 0 up to 10° . Laser vibrometry was used in order to describe the hydrofoil vibratory response. Time Resolved Particle Image Velocimetry (TR-PIV) was also used to visualise the flow and question the origin of the hydrodynamics excitation mechanism. This work aims to describe the different configurations generating strong coupling between the flow and a trailing edge structural eigenmode. It has been shown that vibrations of significant amplitude can be observed for a specific range of angle of attack from 3.5° to 8.5° and that the pressure surface boundary layer separation close to the trailing edge plays a key role in the hydrodynamics excitation mechanism.

Key Words : Fluid-Structure Interaction, Hydroelastic vibration, Trailing-edge flow, hHdrodynamic tunnel

1 Introduction

As it can affect performances, prone structural failures, disturb users, impact acoustic discretion and the whole ecosystem around, noise and vibrations of hydrodynamic lifting surfaces is a matter of great

concern. According to Blake [2] three unsteady flow mechanisms can be responsible for the vibration of hydrofoil operating at low angle of attack. The first one is due the unsteadiness of the incoming flow generating unsteady random hydrodynamic loading and a so-called buffeting response of the hydrofoil. The second can also be referred to as turbulence-induced vibration but due to the boundary layer on the hydrofoil surface. It thus mainly concerns hydrofoil operating at high Reynolds numbers. The third one is due to a tonal flow excitation generated by a periodic vortex shedding from the trailing edge. For hydrofoil with blunt trailing-edge the vortex wake organisation can be regarded as a Kármán vortex street, as for the canonical circular cylinder configuration. But for hydrofoil with sharp trailing-edge, the exact mechanism responsible for discrete frequency organisation of the wake remain unclear. In that context, works done on tonal noise of airfoil in the last decades are of great interest. The first mention of discrete frequency tones from a sharp-trailing-edge airfoil at moderate Reynolds number is probably due to Clark [3]. Paterson *et al.* [9] also mentioned tonal noise on airfoil at Reynolds numbers close to 8×10^5 and a small angle of attack $\alpha = 6^\circ$ and introduced a frequency evolution law based on a constant Strouhal number $St = 0.1 = 2f\delta/U_\infty$, referred to twice the trailing-edge laminar boundary-layer thickness :

$$f = \frac{0,011U_\infty^{1.5}}{\sqrt{c\nu}}, \quad (1)$$

where f is the frequency tone, U_∞ the flow speed and δ the boundary layer thickness at the trailing edge (for either the suction or pressure side), c is the hydrofoil chord and ν the fluid kinetic viscosity. In 1974, Tam [12] questioned the simple Strouhal number correlation and the Kármán vortex type organisation of the wake and proposed that the tones are generated by a self-excited feedback loop involving unstable disturbances in the boundary layer and in the wake flow, along with the feedback of acoustic waves. Using this feedback loop model, a ladder type evolution of the dominant frequency can be drawn that cross the Strouhal law of Paterson *et al.*. Following the work of Paterson *et al.* and Tam, Arbey *et al.* [1] assumed that the ladder-type evolution of the frequency can be due to an aeroacoustic feedback loop involving the diffraction of Tollmien-Schlichting (T-S) instabilities by the trailing edge and the maximum velocity point of the airfoil. In an attempt to clarify the tonal noise generation mechanism on aerofoils at moderate Reynolds number, Nash *et al.* [7] conducted experiments on a NACA0012 aerofoil section. They showed that the ladder type evolution of tones could be eliminated in anechoic conditions. Their results also revealed the presence of strongly amplified boundary-layer instabilities just upstream of the pressure surface trailing edge that roll up to form a regular Kármán-type vortex street. They proposed a new mechanism for tonal noise generation based on the growth of T-S instability waves amplified by inflectional profiles in the separating laminar shear layer on the pressure surface. In another paper, the same team [6] concentrates their work on the stability of pressure side boundary layer in a way to understand the relationship between T-S waves and tonal noise. They conducted experiments on two aerofoil, including an asymmetrical one, which permit to show the impact of airfoil shape on the tonal noise frequency. They also confirmed that tonal noise is closely dependent of the presence of laminar separation bubble on the pressure side close to the trailing edge. In 2007, Nakano *et al.* [8] carried out experiments allowing to clarify the impact of the angle of attack on the tonal noise mechanism at moderate Reynolds number $Re = 1.6 \times 10^5$. Using liquid-crystal visualisation and particle image velocimetry, they confirmed that a laminar separation bubble move along the foil in both the suction and pressure side as a function of the angle of attack. They also showed that the tonal noise apparition is strongly link to the location of the reattachment point of the LSB near the trailing edge on the pressure

side at low angle of attack.

More recently, Probsting *et al.* [10] investigated on a NACA0012 airfoil emitting tonal noise. They found that for an angle of attack of 1.2° and for $Re \leq 4.5 \times 10^5$, tonal noise emission could also be due to an acoustic feedback involving a laminar separation bubble (LSB) formed on the suction side of the airfoil. These different studies did not take into account the hydrofoil vibrations. Conversely Ducoin *et al.* [5] observed discrete frequency excitation mechanism involving a laminar separation bubble on the suction side of an hydrofoil thanks to vibratory response. Based on experiments conducted on a NACA66312 laminar hydrofoils at low angles of attack and transitional Reynolds numbers, they showed that the frequency of the boundary-layer transition mechanism can couple with some natural frequencies of the hydrofoil leading to significant vibrations.

Following those works, the aim of the present study is to clarify, on a symmetric NACA0015 hydrofoil operating at moderate Reynolds numbers, the configurations leading to strong hydroelastic coupling between the trailing edge flow and a trailing-edge mode of the hydrofoil. The experimental set-up along with the hydrofoil modal characteristics are presented in Section 2. Results and discussions focussing on the trailing edge vibrations and wake organisation are reported in Section 3, prior to a conclusion.

2 Materials and methods

Experiments were performed in the hydrodynamic tunnel of the French Naval Academy Research Institute (IRENav) in a square test section of 0.192×0.192 m having a honeycomb standardized inlet flow (figure 1). An Aluminium NACA0015 section hydrofoil of 69GPa Young modulus, constant chord of 0.1m and a span of 0.191m was mounted in a clamped-free configuration. The flow speed was regulated in a range of 2 to 9 ms^{-1} (i.e. a Reynolds numbers range, referred to the chord, from 2×10^5 up to 9×10^5).

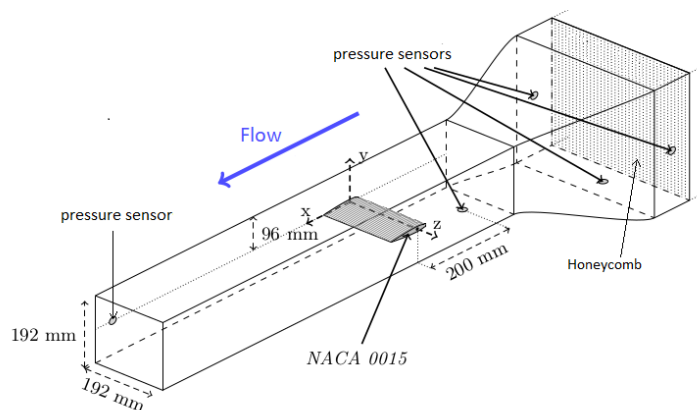


FIGURE 1 – Clamped-free hydrofoil model in the IRENav Hydrodynamics test section

Vibration measurements of the hydrofoil were performed in a point located at 70% of the chord and 64% of the span with a PSV-400 vibrometer that operates thanks to doppler-effect with a 10 ms^{-1} minimum precision. The sensor was disassociated from the tunnel structure in order to limit the impact of pump vibrations. A reflected patch of 3M® S80 film was used on the profile to increase the signal quality.

Eigenmodes of the hydrofoil were determined with the vibrometer using a scanning mode technique and exciting the model with a vibrating pot at a frequency of 1Hz in still water. Fifty five points were used to mesh the profile and determine the phase in order to reconstruct the deformation. Eigenmode frequencies

are reported in figure 2. For result reliability and avoid spectral overlap, all vibration spectrum were calculated with Fast Fourier Transform on an average of 16 data sample of 1s at a frequency acquisition of 9,6kHz. The eigenmodes spatial deformation associated with the fourth mode, at 845Hz, is show in figure 3. This mode is not the dominant one in still water (see figure 2), but it is the one exhibiting the higher amplitude of vibration in the Reynolds number range explored in the present study. As it can be seen in figure 3, this mode has an area of high deformation close to the trailing edge with a maximum at mid-span. This 845Hz eigenmode, labeled "mode 4", is then called a flapping trailing edge mode.

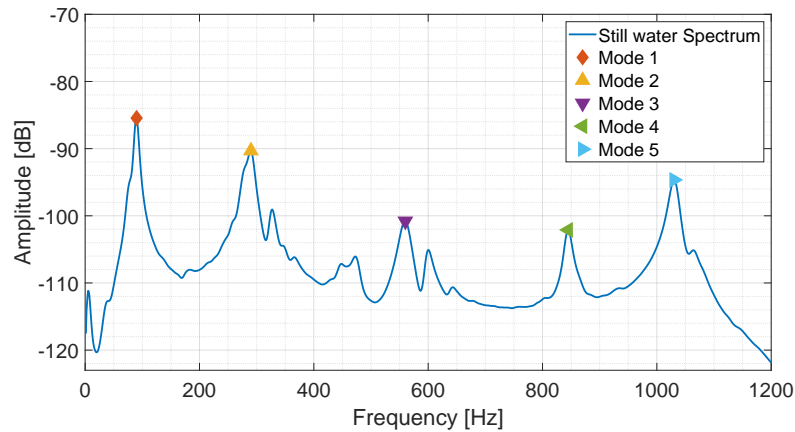


FIGURE 2 – Quiet water hydrofoil eigen frequencies

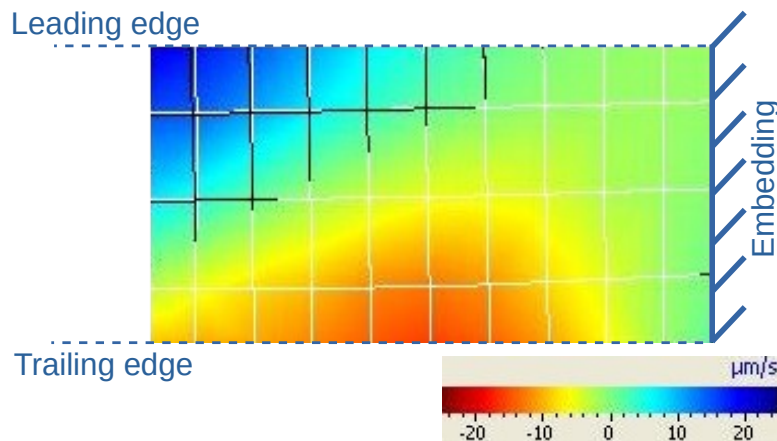


FIGURE 3 – Mode 4 (845Hz) deformation shape

Particle Image Velocimetry (TR-PIV) was done with a SpeedSense 2640 Phantom camera and a 1024x400 pixel frames at 10 000Hz. DynamicStudio® from Polytech® post processing was performed with interrogation area of 16x8 pixel and 4 pixel recovery giving rise to 251x98 pixel vector fields. For each acquisition, 2000 pictures were collected.

Dynamic mode decomposition (DMD) was performed in order to identify wake coherent structure. Schmid *et al.* [11] showed that DMD method is able to extract dynamic information from experimental flow and can be used to describe the physical mechanism. DMD reconstruction presented in this article are spatial TR-PIV flow speed vector associated to the frequency exhibiting the highest spatial consistency.

3 Results and discussions

3.1 Trailing edge vibrations

Trailing edge vibratory responses have been measured for the hydrofoil having different fixed root angle of attack (from 0 up to 10°) and varying the incoming velocity from 2 to 9 m s^{-1} (i.e. a Reynolds numbers range from 2×10^5 up to 9×10^5). Results have shown that trailing edge vibrations occurred for specific range of angle of attack $3.5 \leq \alpha \leq 8.5^\circ$. Amplitude and frequency of the dominant peak in the response spectrum, for $\alpha = 8^\circ$, are reported in figure 4 as a function of the Reynolds number. At low Reynolds numbers $3 \times 10^5 \leq Re \leq 6 \times 10^5$ the dominant peak in the response spectrum is the one associated to the first bending mode of the hydrofoil. The slight increase of the amplitude response in this Reynolds number range can be attributed to turbulence-induced vibrations due to the residual turbulence of the incoming flow. A significant increase of the amplitude response can be observed for $Re \geq 6 \times 10^5$ along with a switch to a frequency close to the one of the flapping trailing edge mode (mode 4). It is interesting to note that the observed lock-in frequency is slightly lower than the one observed in quiet water. That can be explained by the impact of added hydrodynamic stiffness on the fluid-structure eigenmodes. Using the Strouhal law of Paterson *et al.* (equation 1) a lock-in between the vortex wake organisation and the flapping trailing edge mode is expected for $Re \approx 8 \times 10^5$ which is consistent with those results.

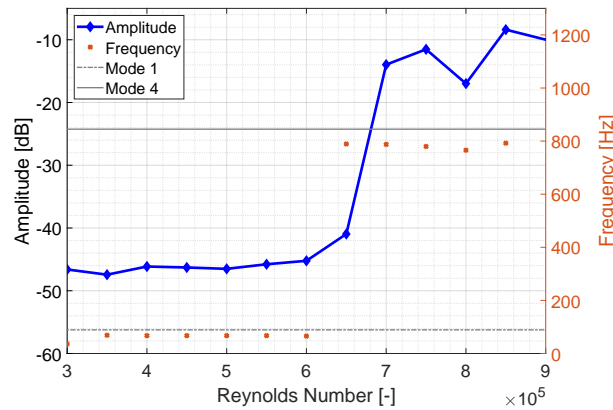


FIGURE 4 – Amplitude and frequency of the dominant peak in the response spectrum as a function of the Reynolds number, for $\alpha = 8^\circ$.

Amplitude and frequency of the dominant peak in the response spectrum, for $Re = 8 \times 10^5$, are reported in figure 5 as a function of the hydrofoil root angle of attack. For angle of attack lower than 2° , vibrations of low amplitude are observed at frequency close to the one of the first bending mode. A slight increase of the response is observed for $\alpha = 2.5^\circ$. Investigations are ongoing to clarify that point. Between 3.5° and 8.5° the dominant peak frequency switches to a frequency close to the one of the flapping trailing edge mode (mode 4) and a huge bump can be observed in the amplitude of vibrations, with a maximum observed for $\alpha = 7^\circ$. Slight frequency variations can be observed. In particular, the coupling frequency slightly decreases with the angle of attack between 6° and 8.5° . For $\alpha \geq 9^\circ$ the hydrofoil vibration is, again, dominated by turbulence-induced vibrations, involving the first bending mode.

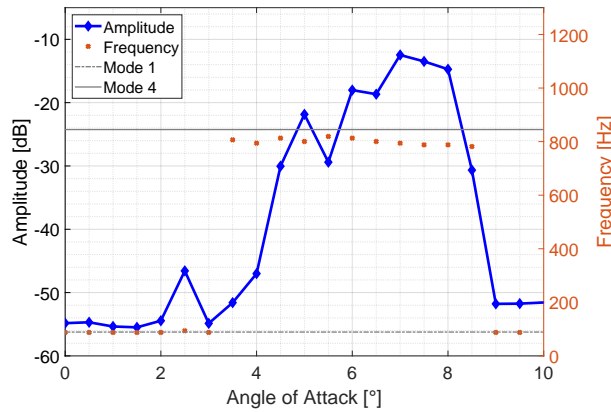


FIGURE 5 – Amplitude and frequency of the dominant peak in the response spectrum as a function of the hydrofoil root angle of attack, for $Re = 8 \times 10^5$.

3.2 Wake Analysis

Time Resolved Particle Image Velocimetry (TR-PIV) was used to visualise the flow and question the origin of the hydrodynamics excitation mechanism. Results presented here concern the hydrofoil with a root angle of attack of 8° and a Reynolds number of $Re = 8 \times 10^5$ for which strong coupling has been observed. TR-PIV measurements, when the resolution is correct, can be used as local unsteady probes to catch the flow variation in both intensity and direction. Figure 6 presents the frequency of the dominant peak associated to the local velocity spectrum. Time evolution of each flow speed is analyzed in Fourier space and the maximum frequency pic is displayed. Left corner square represent the trailing edge of the hydrofoil were pressure side is on the bottom and suction side is not illuminated by laser. A $f \approx 740Hz$ frequency pattern is clearly present in the wake. It is interesting to note that this pattern appears slightly before the trailing edge (96% of the cord) on the pressure side, while it appears significantly forward the trailing edge in the suction side. An interface is also clearly visible between the upper and lower area, suggesting a Kármán-type vortex street.

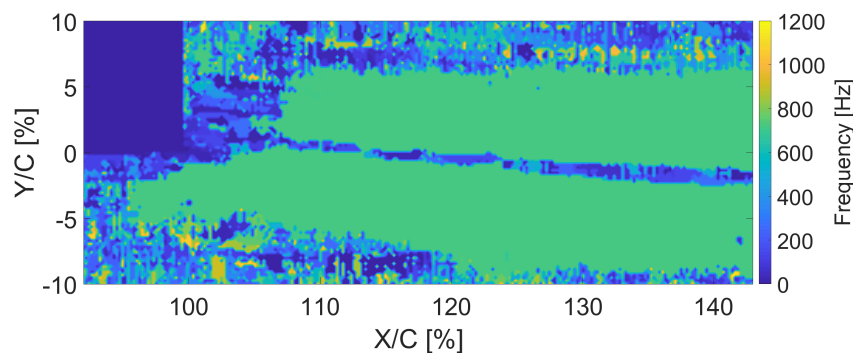


FIGURE 6 – Frequency of the dominant peak associated to local velocity spectra; for $Re = 8 \times 10^5$ and $\alpha = 8^\circ$

Dynamics Mode Decomposition was also performed [13] in order to clarify the associated fluid mode shape. A $f \approx 770Hz$ pattern was found. Results are shown on figure 7. The frequency associated to this coherent wake organization is slightly different from the one identified previously from spectral

analysis and also slightly lower than the one observed from the hydrofoil trailing edge mode vibrations. Conversely, the same method was performed for an angle of attack equal to 9° for which no trailing edge vibrations were observed (see figure 5). No dominant frequency appears in the wake and the DMD method does not detect any coherent pattern.

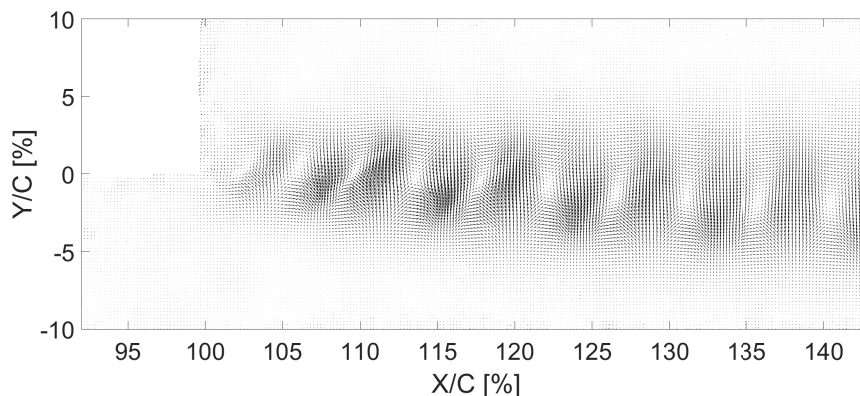


FIGURE 7 – $f \approx 770\text{Hz}$ pattern identified from dynamics mode decomposition; for $Re = 8 \times 10^5$ and $\alpha = 8^\circ$

3.3 Discussions

The extension of a coherent wake flow frequency pattern on the pressure side slightly upstream the trailing edge, clearly suggests that an hydrodynamic phenomenon involving a pressure side amplification of the shear layer separation is at the origin of a coupling with the so-called trailing edge mode 4 of the hydrofoil. The dynamic mode decomposition also highlights a well organized vortex shedding structure when the trailing edge mode of the hydrofoil is coupled with this trailing edge flow. The fact that strong coupling has been observed for a specific range of angle of attack $3.5^\circ \leq \alpha \leq 8.5^\circ$ is also consistent with the work of Nakano *et al.* [8] and reinforces the hypothesis that the state of the boundary layer on the pressure side of the hydrofoil, close to the trailing edge, is a key parameter. The coupling should then be optimum when the reattachment point of a laminar separation bubble and/or transition point is close to trailing edge. An XFOIL solver [4] analysis of the NACA0015 boundary layer evolution also confirmed that the transition point, on the pressure side, gradually moves forward the trailing edge with the angle of attack. For angles of attack less than 3.5° the transition point is too far upstream the trailing edge to have any effect and for angle of attack above 8.5° the transition does not occur on the pressure side. This could also explain the gradual rise in amplitude of the vibratory response as the transition point get closer to the trailing edge with the angle of attack increasing (figure 5).

4 Conclusion

Trailing-edge vibrations on a NACA0015 hydrofoil was experimentally investigated. A hydrodynamics excitation mechanism was also questioned based on unsteady wake analysis and previous work done on airfoil. A strong coupling with the mode 4 is observed for a narrow range of angles of attack. This eigenmode mode is a trailing edge deformation one. It was also shown that sufficient flow speeds are necessary for trailing edge flow-induced vibrations and that the lock-in can be predicted using a frequency evolution law based on a constant Strouhal number. The dynamic mode decomposition has highlighted a well organized vortex shedding structure when the trailing edge mode of the hydrofoil is coupled with

this trailing edge flow. The unsteady flow analysis also suggests that the location of the boundary layer transition on the pressure side of the hydrofoil is a key parameter. According to previous study it should be close to the trailing edge to enhance the trailing edge flow excitation mechanism. Further work are ongoing to clarify that point.

Références

- [1] H. Arbey, J. Bataille, Noise generated by airfoil profiles placed in a uniform laminar flow, *Journal of Fluid Mechanics*, 134 (1983) 33–47.
- [2] W.K. Blake, Excitation of plates and hydrofoils by trailing edge flows. *Journal of Vibration, Acoustics, Stress, and Reliability in Design*, 106 (1984) 351–363.
- [3] L.T. Clark, The radiation of sound from an airfoil immersed in a laminar flow, *Trans ASME A : Journal of Engineering Power*, 93 (1971) 366–376.
- [4] M. Drela, XFOIL : An analysis and design system for low Reynolds number airfoils, in *Low Reynolds number aerodynamics*, 1–12, Springer, 1989.
- [5] A. Ducoin, J.-A. Astolfi, M.-L. Gobert, An experimental study of boundary-layer transition induced vibrations on a hydrofoil, *Journal of Fluids and Structures*, 32 (2012) 37–51.
- [6] A. McAlpine, E.C. Nash, M.V. Lawson, On the generation of discrete frequency tones by the flow around an aerofoil, *Journal of Sound and Vibration*, 5 (1999) 753–779.
- [7] E.C. Nash, M.V. Lawson, A. McAlpine, Boundary-layer instability noise on aerofoils, *Journal of Fluid Mechanics*, 382 (1999) 27–61.
- [8] T. Nakano, N. Fujisawa, Y. Oguma, Y. Takagi, S. Lee, Experimental study on flow and noise characteristics of NACA0018 airfoil, *Journal of Wind Engineering and Industrial Aerodynamics*, 7 (2007) 511–431.
- [9] R.W. Paterson, W. Robert, P.G. Vogt, M.R. Fink, C.L. Munch, Vortex noise of isolated airfoils, *Journal of Aircraft*, 5 (1973) 296–302.
- [10] S. Pröbsting, S. Yarusevych, Laminar separation bubble development on an airfoil emitting tonal noise, *Journal of Fluid Mechanics*, 780 (2015) 167–191.
- [11] P.J. Schmid, Dynamic mode decomposition of numerical and experimental data, *Journal of fluid mechanics*, 656 (2010) 5–28.
- [12] C.K.W. Tam, Discrete tones of isolated airfoils, *The Journal of the Acoustical Society of America*, 6 (1974) 1173–1177.
- [13] F. ZGUNOV, Dynamic Mode Decomposition [DMD] - Wrapper, *MATLAB Central File Exchange*, (2021).